HISTORICAL SEISMOLOGIST

The 1892 Chaman, Pakistan, Earthquake

by Roger Bilham, Najeeb Ullah Kakar, Din Mohammad Kakar, Kang Wang, Roland Bürgmann, and William D. Barnhart

ABSTRACT

The >1000-km-long transform fault defining the continental western boundary of the Indian plate (Fig. 1) is named after the town of Old Chaman (30.85° N, 66.52° E) that was damaged by an $6.5 < M_w < 6.7$ earthquake there in 1892 (Griesbach, 1893). We quantify slip and afterslip in the 1892 earthquake from historical reports of rail offsets and rotation, and estimate rupture length from survey reports. We estimate that total slip exceeded 1 m, similar to the current potential slip deficit now prevailing on the fault derived from recent Interferometric Synthetic Aperture Radar and Global Positioning System studies. As a consequence, a recurrence of the 1892 earthquake could soon occur. In 1892, the population of Chaman numbered less than 1000. The present population of Chaman and nearby villages exceeds 0.5 million.

INTRODUCTION

Three major left-stepping faults accommodate most of the left-lateral slip of the Chaman fault system: the Chaman, Ghazaband, and Ornach-Nal faults (Fig. 1), with geodetically estimated slip rates of the order of 15–19 mm/yr, significantly less than the calculated 27 mm/yr plate-boundary slip vector at this longitude (Szeliga *et al.*, 2012). Geological estimates of slip rates on the Chaman fault vary from 19 to 24 mm/yr (Lawrence *et al.*, 1992), with one anomalously high estimate of 33 ± 3 mm/yr near latitude 30° N (Ul-Hadi, Khan, Owen, and Khan *et al.*, 2013). South of Chaman, these major faults are weakly transpressive, resulting in an ≈7 mm of convergence in the ≈180-km-wide Kirthar ranges, a fold-and-thrust to their east associated with moderate thrust seismicity. North of Chaman, the strike of the transform system veers to the north-northeast and averages ≈30° oblique to the plate slip vector, resulting in a doubling in the width of the fold-and-thrust belt (Haq and Davis, 1997). The average present-day convergence rate absorbed by fold belts east of the Chaman fault is ≈13 mm/yr (Szeliga *et al.*, 2012).

In 1505 and 1519, major earthquakes occurred on the northernmost segments of the Chaman fault in Afghanistan, but in historical and recent times, sinistral earthquakes on the Chaman fault south of 33° N have not exceeded M_w 6.8 (Ambraseys and Bilham, 2003a,b; Ambraseys and Douglas, 2004). Interferometric Synthetic Aperture Radar (InSAR) analysis has revealed the presence of surface creep and afterslip following $M_w > 5$ earthquakes on the Chaman fault (Furuya and Satyabala, 2008; Szeliga *et al.*, 2012; Barnhart, 2017; Crupa *et al.*, 2017), and a prominent shear field of 16 ± 2 mm/yr has been associated with the Ghazaband fault (Fattahi and Amelung, 2016).

Despite the morphological prominence of the Chaman and Ghazaband faults, the largest earthquake in the past 200 yr to release sinistral slip along India's western transform system was the M_w 7.7 earthquake that destroyed Quetta on 31 May 1935 (West, 1935). Surface rupture occurred on an unnamed surface fault subparallel to the Ghazaband fault and approximately 30 km to its east, terminating near Quetta. The length of the causal 1935 rupture is inferred from its mainshock–aftershock distribution to exceed 100 km, and the mean slip inferred from its magnitude may have approached or exceeded 4 m. Sinistral slip near the northern end of the 1935 surface rupture did not exceed 1 m, as estimated from the buckled rail line crossing the fault near Mastung (Skrine, 1936, PLate3). Field visits to this location in 2019 (29.894° N, 66.818° E) revealed that villagers have retained a collective memory of 1935 surface fissuring, damage to dwellings, and fatalities in villages located along the nearby fault scarp.

THE 1892 EARTHQUAKE

At 05:40 IST (≈00 : 19 GMT) on 20 December 1892, an earthquake occurred on the Chaman fault. No deaths were reported, although considerable damage occurred in the town of Chaman on the Afghan border and in villages on the road between Kandahar and Quetta. The only known surviving photograph of structures affected by the earthquake is reproduced by Egerton (1893), which shows buildings of the public works department still standing at Old Chaman (30.859° N, 66.523° E) within 10 m of the fault trace (Fig. 2). A week after the earthquake, at the railway station of Sanzal (32.826° N, 66.519° E) 0.7 km from the fault, Griesbach relates, "The water tower is standing, but most of the turrets are loose. The oscillation of the ground caused the water to spill out of the iron tanks. The station building including the station master's and signaler's quarters and

doi: 10.1785/0220190148

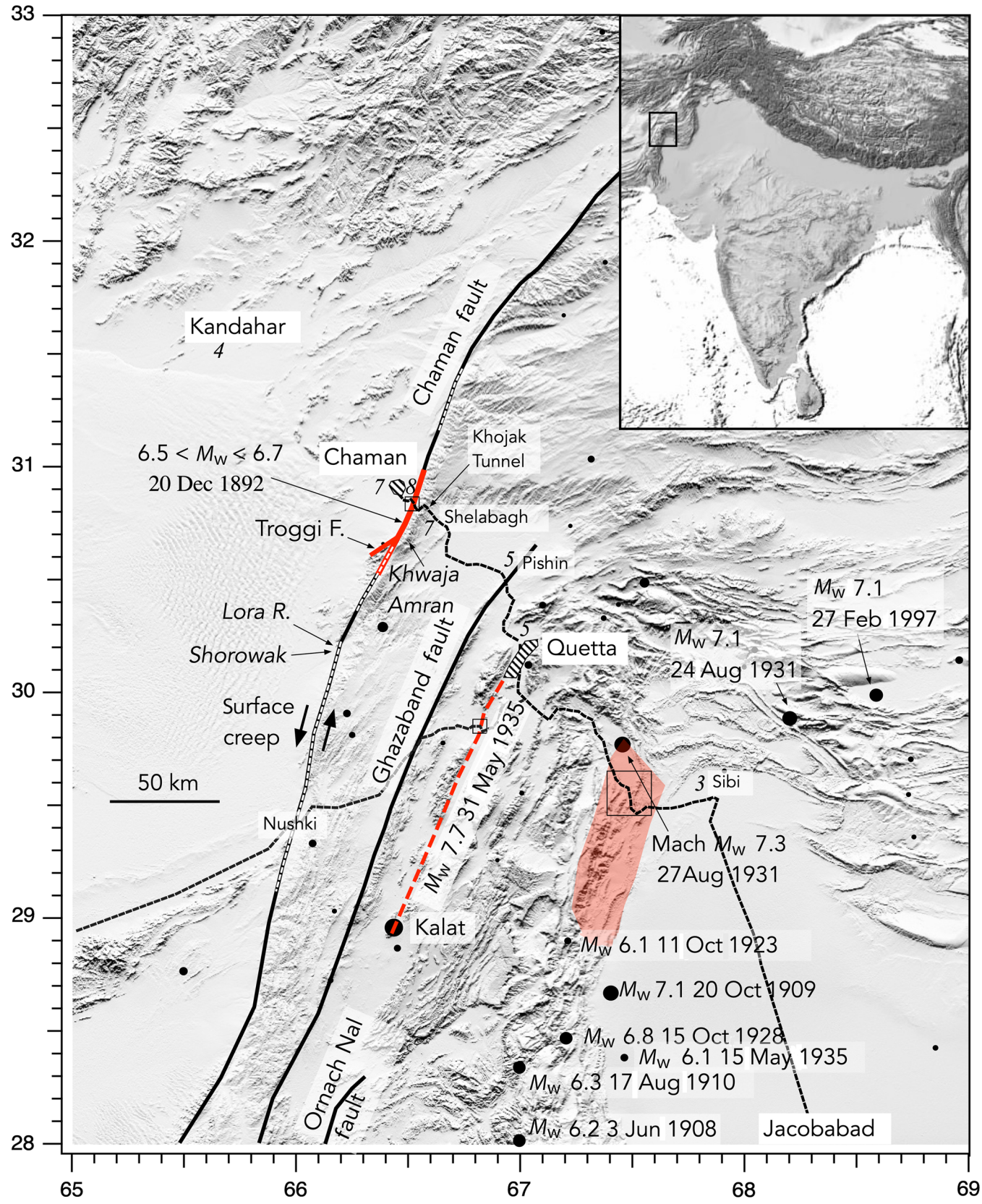

▲ **Figure 1.** Location map showing recent ruptures (red) and significant earthquakes 1892–2019. (Inset) Location of main figure. Shaking intensities reported in the 1892 earthquake are indicated in italics. White dashed lines indicate surface creep; black dashed lines indicate railroads; open squares indicate three locations where coseismic slip has been constrained by railroad deformation in 1892, 1931 (Szeliga *et al.*, 2009), and 1935. The color version of this figure is available only in the electronic edition.

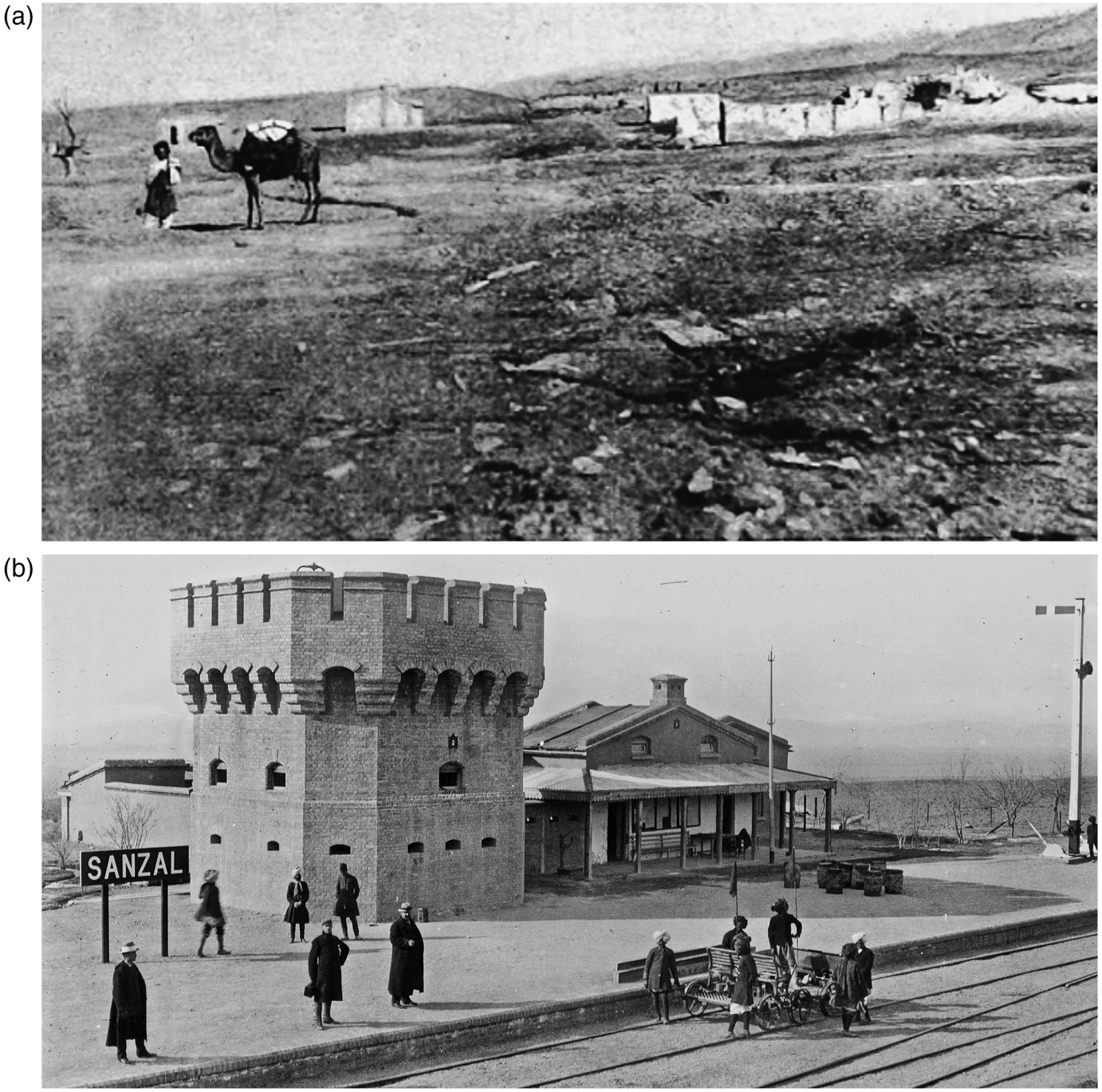

▲ **Figure 2.** (a) North-northeast view of the Chaman rupture of 1892 showing the mole track of the surface rupture running from the foreground to the distance between structures in Old Chaman (Egerton, 1893). Some roof collapse may have occurred to structures within 30 m of the fault (intensity 7 < EMS < 8). (b) View of Sanzal station (700 m from the fault) repaired 3 yr after the earthquake (Jackson, 1895). The tessellated masonry structure supports an open water tank. EMS, European Macroseismic Scale.

out-houses are very badly shaken, and will require rebuilding to a considerable extent. The whole of the chimneys have been thrown down" (Fig. 2). Stone defensive towers at the west entrance of the Kojak tunnel (30.853° N, 66.555° E) were cracked but not those at the east portal (30.832°, 66.588° E) near Shelabagh (Shalabagh) where poorly constructed dwellings collapsed. The tunnel is 3.9 km long, and work on the tunnel lining was in progress during the weeks following the earthquake. No damage occurred to the lining, but workers were reportedly frightened by aftershocks for the next two months. Felt effects lessened along the path of the railway and road toward Quetta, which provides a linear view of shaking strength variation roughly normal to the fault. The earthquake was not felt outside Balochistan. From these and from limited instrumental data,

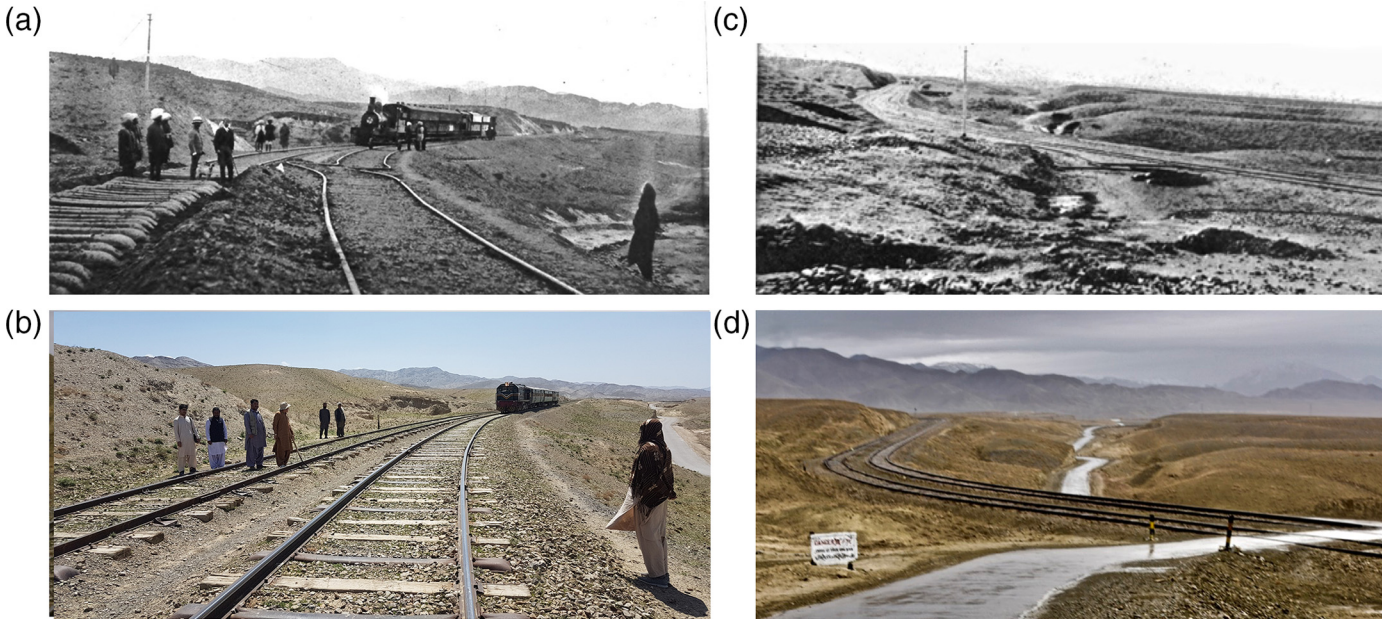

▲ **Figure 3.** Southward views of the railroad crossing the Chaman fault in (a,c) December 1892 and in (b,d) February 2019. In 1892, the standard 24 ft segments of rail track were shortened by 69–76 cm to accommodate fault movement. The line lengths were apparently further shortened ≈30 cm to accommodate additional afterslip. See Figure 4 for map of the viewpoints of the photographs. Visible in (c) are discarded bent rails near repaired track and a view of the straight segment of rail entering the bend from the south (see Fig. 5). The color version of this figure is available only in the electronic edition.

Ambraseys and Bilham (2003a,b) assign the earthquake a magnitude of $6.5 < M_s < 6.7$.

Two photographs of the Chaman–Quetta railroad where it crosses the fault obliquely in compression (Fig. 3) were taken by L. Gordon, the railway engineer responsible for repairs, and these were reproduced by both Griesbach (1893) and Egerton (1893). The first shows a view of the rails in a southerly direction with the eastern pair of rails removed and the western pair of rails crumpled, and the second shows a view of the fault trace in a south-southwest direction following the repair of both lines, with the discarded damaged rails north of the track. Griesbach (1893) and Egerton (1893) also provide map views of the buckled lines (Fig. 4), which show the eastern rail apparently more crumpled than the western rail. An ≈400 m radius bend in the rails where they cross the fault causes the eastern outer rail to cross obliquely at 19° and the western inner rail to cross at 16°.

The standard rail lengths in Balochistan were multiples of 6 or 10 ft, and present-day dimensions with different lengths are symptomatic of rails truncated to accommodate fault slip. Griesbach (1893) relates that following the earthquake, 43.89 m of crumpled rails in the western down line were removed (four 20 ft, plus one 24 ft) and replaced with 43.13 m of fresh rail (five 24 ft, plus one 21.5 ft). The 21.5 ft anomalous segment mentioned implies a shortening of 2.5 ft (76.2 cm) to accommodate fault slip. Egerton (1893), the engineer in charge of the railway, reports, however, that the line was shortened by 2.25 ft (69 cm), implying the anomalous rail segment length was not 21.5 ft but 21.75 ft long. These two measurements may be reconciled by assuming that they correspond to the shortening needed for the outer and inner rails of the curved track. We remeasured the rail lengths near the fault in 2019 and found two rail lengths of 20.31 and 21.04 ft that possibly represent the original 1892 rails further shortened by 0.71 and 1.2 ft, respectively (29 ± 8 cm), an amount that we tentatively ascribe to accommodation of 31 ± 8 cm of sinistral afterslip on the fault subsequent to the 1892 repairs (after correcting for the ≈19° obliquity of the rails to the fault).

Marring the confidence of this simple conclusion, however, is the existence of an inexplicable 13.94 ft segment not mentioned in historical accounts, contiguous with the aforementioned 20.31 ft segment on the eastern track. We unsuccessfully sought independent evidence for fault slip from the western track. The present-day segment lengths of the western track within 150 m of the fault, however, were found to consist of 42 ft long segments (with one 40 ft segment length), suggesting these were replaced relatively recently, and that creep processes on the fault since their replacement have been minimal. Discussions with the track maintenance engineers were unable to elucidate the times of repairs to the track or the timing of the western track replacement, although they suggested this may have occurred in 1936 at a time of major work to the lines. The track engineers were adamant that no recent repairs have been necessary other than the routine fish-plate tightening and sleeper renewal of the sort typically needed on a curved gradient subject to significant forces from descending trains. If true, this implies that creep since 1936 has been less than a few centimeters, an amount that can be accommodated by fish-plate contraction without rail-segment shortening.

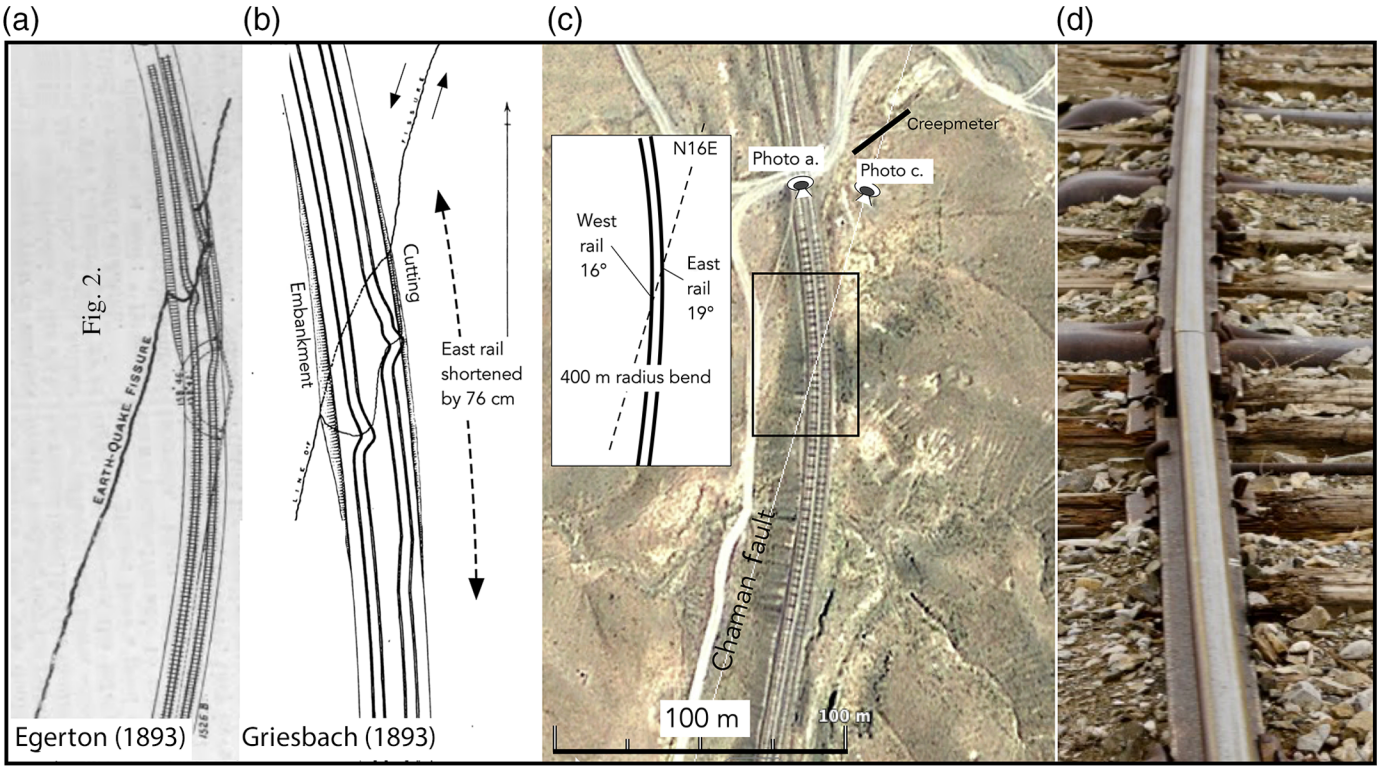

▲ **Figure 4.** Crumpled rails at 30.853° N, 66.519° E before repair according to (a) Egerton (1893) and (b) Griesbach (1893). Egerton shows a coseismic 46 cm southward movement of the intersection of the straight rail segments outside the curve and a 1.2 mrad reduction in the obtuse angle between them. (c) Google Earth 2010 view of fault geometry showing the viewpoints of the two photographs in Figure 3 and location of a new creepmeter. (d) 2019 southward view of penultimate western rail with fish-plate joint where it crosses the fault. Incipient buckling and the absence of expansion gap are consistent with minor recent fault creep. The color version of this figure is available only in the electronic edition.

Egerton (1803) concludes his account of coseismic rail shortening by indicating that the projected intersection of the distant straight line segments of rail approaching the bend was shifted southward (on the east side of the fault) by ≈46 cm and the obtuse angle between them reduced from 158°46′ to 158°42′ (a decrease of 1.16 mrad). In laying out curves between straight segments of railroad, it was customary to identify the virtual point of intersection of contiguous straight rail segments (i.e., point B in Fig. 5a) and to construct a curve of suitable radius to meet these lines tangentially (Baker, 1850). The railroad had been completed just 5 yr before the earthquake, and it is probable that the preseismic intersection point (a survey-marker driven into the ground at point B) was still in position for Egerton to be able to quantify the reduction in angle ABC precisely as 1.16 mrad. He presumably used the alignment BC as a reference azimuth because B and C both lie on the east side of the fault. What remains uncertain, however, is the location of point A in his observation. Quantitative reasoning suggests that instead of measuring angle ABC in Figure 5a, Egerton measured the angle A′B′C (Fig. 5d), in which A′ was a survey target on the AB segment of the rail, and B′ was the newly shifted position of marker point B relative to the west side of the fault zone.

Elastic models for surface deformation accompanying 70 cm of slip on the Chaman fault are shown in Figure 5b with rupture terminating at different depths in the subsurface. Although deformation is approximately antisymmetric about point B in these models, the larger angle of AB to the fault (26.6°) rotates significantly more coseismically than BC (the southward-trending segment receding into the distance in Fig. 3c). The angular reduction in ABC accompanying rupture is a function of the shallowness of rupture (blue curve in Fig. 5c), the amount of slip on the fault, and the distance of point A from the fault. However, for reasonable values of subsurface fault slip (<3 m), it is not possible to match Egerton's observed 1.16 mrad angular reduction in ABC. For such a large angular change, surface rupture is necessary, and Egerton would have needed to observe angles to a point A′ located no more than ≈142 m from the fault, or ≈160 m from the fault along the railroad segment AB. In Figure 1d, we show a geometrical condition that satisfies the fault slip inferred from rail shortening (≈76 cm), Egerton's observed 46 cm southward movement of the postseismic intersection of AB and BC, and his 1.16 mrad reduction in the angle A′B′C′. Were point B precisely centered in the fault zone, it would have appeared to move 38 cm south relative to the line of sight AB for 70 cm of fault slip. Its greater motion relative to

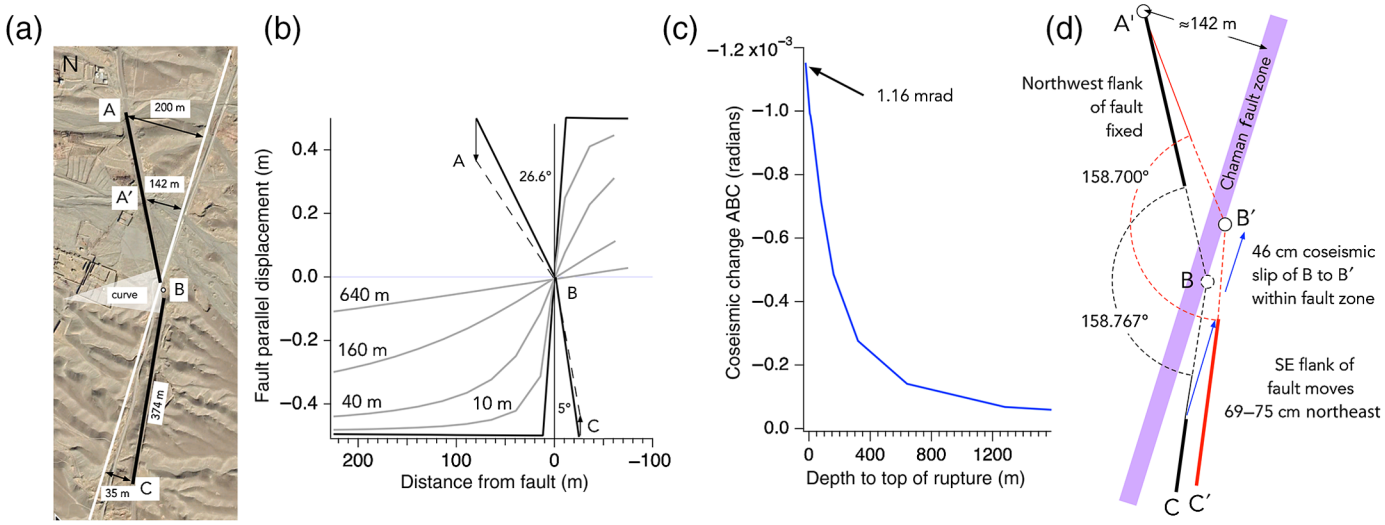

▲ **Figure 5.** (a) Map view of fault and point B used to lay out curve. (b) Surface deformation versus flank distance for coseismic slip terminating at the surface and at indicated subsurface depths. (c) Variation in angle A′BC for subsurface slip shown in (b) for a point A′, on line AB, 142 m from the fault. (d) Map view of reported displacements and angle changes holding the west flank of fault fixed, illustrating Egerton's inferred angular change A′B′C–ABC (not to scale). The color version of this figure is available only in the electronic edition.

the west side of the fault occurs because B is located less than 20 m east of the center of the fault zone. However, the important conclusion from this analysis (Fig. 5) is that 70 cm of fault slip in 1892 appears to have been manifest as block-like motion near the fault.

This presents an interpretational difficulty for, as noted by Davison (1893), had block motion occurred, the azimuths of previously straight segments AB and BC would not have changed. This contradiction is reconciled earlier by proposing that Egerton measured the postseismic angle A′B′C′ and compared its value with the preseismic angle ABC (Fig. 5d).

Griesbach (1893) estimates that 20–30 cm of subsidence occurred to the west of the fault, whereas Egerton (1893) ventures just 10 cm, and Davison (1893) reports 5 cm from repeated spirit leveling. Faulting down to the west results in extension of the rails, and hence the observed shortening must be increased by $(L^2 + 0.2^2)^{0.5} - L$ m, in which L is the length of the track descending the fault scarp. We estimate 25 m $< L <$ 50 m, and hence, this correction is negligible (≤1 mm).

A few inconsistencies occur in the 1892 accounts that we dismiss as errors in reporting. In Egerton's article, the topographic scarp height (14 ft) was mistakenly equated with coseismic dip-slip movement, and the photographed location of the surface fault, which we reproduce in Figure 2a, was incorrectly described in its figure caption, errors that we attribute to misunderstandings in correspondence received by the publisher. An account in the *Railway Review* for Anonymous (1893) stating that both rails were wrecked for more than 600 yards is almost certainly a misprint for 600 ft, approximately equivalent to the total lengths of steel replaced and realigned on the two tracks.

The 46 cm offset in the alignment of contiguous straight segments where they enter the bend reported by Egerton (1893) in principle provides a direct measure of fault slip, but in practice is rendered uncertain by point B being within the fault zone (Fig. 5). If 76 cm of shortening occurred on the rail at 19° to the fault, we obtain a maximum value for left-lateral fault slip of 76/ cos 19° = 80 cm. Using minimum values for rail shortening and obliquity, we obtain a minimum estimate of 69/ cos 16° = 72 cm. In what follows, we adopt a value for left-lateral slip of 76 ± 4 cm in the first week following the earthquake, with subsequent afterslip of 31 ± 8 cm that was probably complete within a few years after the earthquake.

RUPTURE LENGTH 1892

The full extent of the 1892 rupture length was never mapped. Griesbach followed the rupture personally for a few kilometers to the north and south and explains that it continued as far as he could see into the distance. Egerton (1893) indicates it extended northward beyond the Afghanistan border, that is, 14 km north-northeast of the railroad crossing. Griesbach (1893) learned of its southerly extent from Gordon, who had instructed workers to follow the rupture 34 km to the south of the railway. They reported that the rupture bifurcated to pass on either side of the summit of Khwaja Amran (30.59° N, 66.35° E) where they lost the surface cracks beneath a veneer of snow. We assume the bifurcation signified that slip occurred both on the Chaman fault and on the Troggi fault (Fig. 1), a thrust splay to the west of the Chaman fault described by Lawrence and Yeats (1979). Thus, the rupture length apparently exceeded 48 km.

A further observation of the Chaman surface rupture was made a few years after the earthquake by McMahon and Holdich, who were mapping the Afghan boundary. McMahon (1897, pp. 402–403) states that they "carefully mapped ... this wonderful earthquake crack" (Fig. 6) starting 32 km north of Chaman extending southward 216 km to Nushki, beyond which

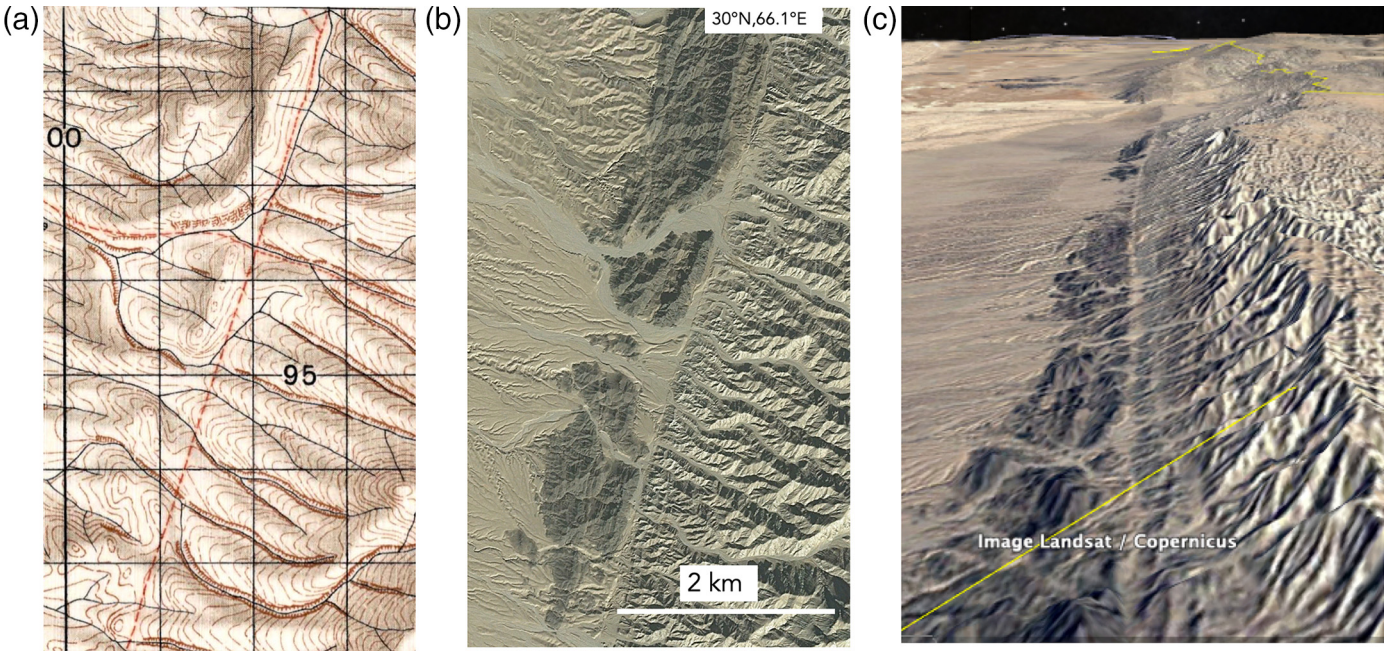

▲ **Figure 6.** (a) "Wonderful earthquake crack … as clearly defined as a railway cutting" dashed red in McMahon's map as a track 25 km north of Nushki (Burrard, 1915; Wheeler, 1941). (b) Google Earth view of the same location. (c) Vertically exaggerated Google Earth view north, with the fan of the Lora River in the background where it debouches into the plains near Shorowak. Left-lateral offsets are evident in streams crossing the fault, but these were not noted by McMahon or his staff. The color version of this figure is available only in the electronic edition.

they could not follow it. He relates, "[I]t is a well-defined broad line of deep indentation, in places as clearly defined as a railway cutting [Fig. 6]. Along the whole course of it are to be found springs of water, cropping up here and there. Both from the presence of water and from its forming a short-cut across mountain spurs, this crack is largely used as a thoroughfare. We found the old greybeards of the tribes residing in the neighbourhood all know of its existence. They told us that during their lifetime, on some three occasions after severe shocks, deep fissures had appeared along this line, and that they had similar accounts handed down to them from their fathers." Note: The reports of severe shocks experienced by villagers and their ancestors apply to earthquakes in the eighteenth and nineteenth century for which we have no historical record (Ambraseys and Bilham, 2003a,b). The fault gouge acts as an aquiclude, and villages and grazing land are found along the fault where surface springs provide a year-long source of water.

Further information on the fissure was related in dispatches from the McMahon's boundary survey team to the *Times of Bombay* and *The Englishman* of Calcutta (Anonymous, 1909). "Spintijha [Spin Tesa 30.560° N, 66.385° E] is placed at the upper end of a sloping valley, and it derives its name from the existence of a white volcanic rock with some smaller ones adjacent to it. These run along the line of the earthquake crack which has existed probably for centuries, but which was widely reopened in 1892, and has been traced from Murgha Chaman [31.09°N, 66.60°E] as far down as Shorawak [30.18° N, 66.18° E], over 80 miles by Captain McMahon [note: the along-fault distance from Murgha Chaman to Shorowak is approximately 100 km, 28 km less than claimed]. Its direction here is from north-east to south-west, and it apparently terminates in the latter direction in the desert. The remarkable feature of the country is that the hills to the east of the crack are composed of sedimentary rock while those to the west are igneous."

On 4 February 1895, the Baluch–Afghan boundary demarcation surveyors climbed to the summit of Khwaja Amran peak (30.597° N, 66.361° E), and the account continues, "Unfortunately there was too much haze about for the survey officer [G. P. Tate, Survey of India] to take any observations, but he succeeded in taking some photographs, one being of the earthquake crack alluded to in my first letter. Whatever doubt one might have had about this being really an earthquake crack as seen at Spintijha [30.56° N, 66.38° E] was dispelled on seeing it from the top of Khwaja Amran. Its course could be clearly traced north towards Chaman and south towards Shorawak [30.18° N, 66.18° E]." Note: Tate's glass plates in the Survey of India headquarters were recycled following the partition of India and Pakistan.

Two weeks later, the 15 February dispatch describes the southern extent of the surface rupture: "After being traced over 100 miles [note: the along-fault distance between Murgha Chaman and the Lora River is 96 km, 64 km less than that claimed in this account] it descended the slope over the eastern side of the lower end of the Kwajha Amran range and apparently ended in the Lora River" (30.2° N, 66.2° E).

A difficulty with these accounts and McMahon's description of the fault is that no distinction is made between the 1892 rupture and previous earthquake ruptures responsible

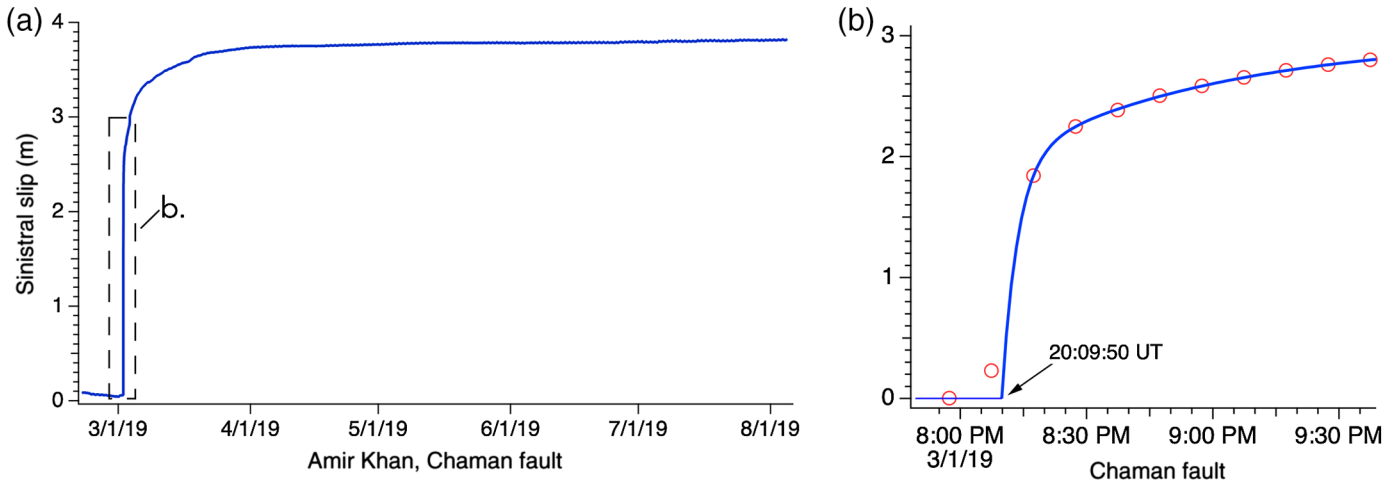

▲ **Figure 7.** (a) A creep event initiated 1 March 2019, 20:09:50 at Amir Khan, 2.5 km northeast of the Chaman rail crossing. (b) Red circled data points are fit to a double exponential decay curve (see Bilham *et al.*, 2016). The preamble preceding fault slip is interpreted to represent strain associated with the approach of a propagating creep event. A second creepmeter was subsequently installed close to the rail crossing (Fig. 4c). The color version of this figure is available only in the electronic edition.

for its pronounced geomorphic expression. That the 1892 rupture was difficult to discern at Spin Teza (30.55° N, 66.38° E) and not traceable across the Lora River fan where it debouches into the plains (30.2° N, 66.2° E in Afghanistan), however, means that 1892 surface rupture did not disturb the recent river gravels, and it thus provides an upper limit for surface faulting of about 68 km. It is probable, however, that the rupture may have been equated with fault morphology for some of this distance and the rupture length did not extend far north of the Afghan border near Chaman, or south of Spin Teza, a distance of the order of 48 km. Lawrence and Yeats (1981) and Yeats *et al.*, (1979) describe the Chaman and Nushki segments of the fault in some detail but also were unable to uniquely identify the 1892 rupture.

We conclude that the southern end of the rupture probably terminated within the restraining bend south of the Troggi fault splay where the Chaman fault traverses the Kwaja Amran range (Ul-Hadi, Khan, Owen, and Khan, 2013). This transpressive bend is responsible for elevations exceeding 2.5 km near the fault and has been the locus of recent minor seismicity.

1892 MAGNITUDE, AFTERSLIP, AND CREEP

From the foregoing discussion, we conclude that the 1892 rupture length may have exceeded 48 km, but was shorter than 68 km, and that surface slip locally amounted to 76 ± 4 cm a week after the earthquake, with possibly 31 ± 8 cm of subsequent afterslip (Table 1). Estimated magnitudes constrained by empirical scaling laws (Thingbaijam *et al.*, 2017) from these rupture lengths correspond to $6.8 < M_w < 7.2$, larger than the intensity-derived magnitude of $6.5 < M_w < 6.7$ (Ambraseys and Bilham, 2003a,b).

The maximum magnitude derived from macroseismic intensity data (M_w 6.7) can be reconciled with the minimum observed rupture length (48 km) if we assume that mean coseismic slip accompanying the earthquake at seismogenic depths was no more than 0.6 m. If this mean slip occurred coseismically at the Chaman rail crossing, the observed slip of 76 cm would imply ≈16 cm of early afterslip prior to railroad repairs to the eastern pair of lines, which took place a week after the earthquake. If we further assume that 23–37 cm of subsequent afterslip continued (as deduced from additional shortening to the eastern track), we deduce that total slip in the earthquake amounted to 1.06 ± 0.07 m. Thus, surface afterslip in 1892 may have approximately doubled coseismic slip at depth. This ratio is similar to the ratio between surface slip observed after a week, and after three years following the 1966 and 2004 M_w 6.0 earthquakes at Parkfield on the San Andreas fault (Lienkaemper and McFarland, 2017). For the Parkfield earthquakes, a total of ≈30 cm of fault slip occurred with a total duration of ≈3 yr.

The western rail track at Chaman indicates that no significant creep has occurred on the fault near the railroad crossing since at least 1936 or perhaps earlier. A creepmeter (Bilham *et al.*, 2016) installed next to the rails in early 2019 has also detected no creep, consistent with recent InSAR imagery, but creep is evident in this imagery at locations to the north and to the south (Szeliga *et al.*, 2012; Fattahi and Amelung, 2016; Barnhart, 2017). A creepmeter 2.5 km north of the rail crossing recorded a 3.8 mm creep event in February 2019 (Fig. 7). This second creepmeter location was selected to be close to an exposure of the fault where villagers had mined the fault gouge for adobe construction materials, and where horizontal slickensides were abundant in the freshly exposed clay gouge (30.8925° N, 66.5334° E).

RENEWAL INTERVAL AND SURFACE CREEP

If we now assume that 1892 slip at the rail crossing in Chaman amounted to 1.06 ± 0.07 m including afterslip, we may

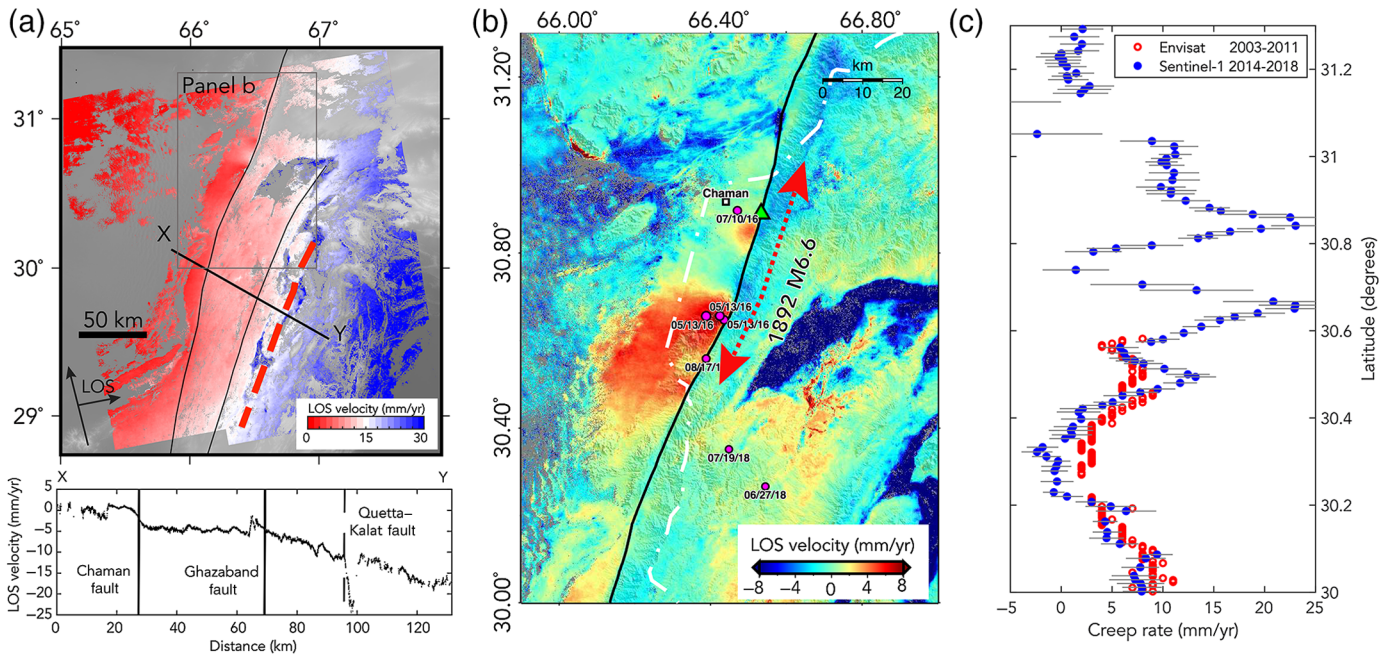

▲ **Figure 8.** (a) 4.5 yr (from October 2014 to March 2019) ascending Sentinel-1 line of sight (LoS) velocity map of interseismic deformation across the Chaman, Ghazaband, and Quetta–Kalat faults. Velocities are in a fixed-Eurasia reference frame; the double arrow indicates the satellite LoS direction. Negative velocities indicate motion away from the radar. Slip in 1935 on the Quetta–Kalat fault was field verified near Mastung in February 2019 but has yet to be mapped southward and hence is shown dashed. The profile *X*–*Y* across the Chaman fault shows a distinctive step of near-surface creep. A shear-strain rate of ≈15 mm/yr is shared by the Ghazaband fault and by the Quetta–Kalat fault. (b) A closer view of recent creep and deformation arising from several M_w 5 earthquakes in 2016 near restraining bends on the fault. The green triangle shows the location of newly installed creepmeters near and north of the rail crossing. Dark blue areas record subsidence resulting from groundwater withdrawal (Khan *et al.*, 2003). Panel (c) quantifies shallow creep rates as a function of latitude along the fault in the period 2014–2018. The color version of this figure is available only in the electronic edition.

proceed to calculate the renewal interval for a repeat of this earthquake. Near Nushki and south of Chaman, the surface creep rate peaks at 8 mm/yr (Fig. 8). A Global Positioning System (GPS) line across the fault near Chaman (Szeliga *et al.*, 2012) has been interpreted to imply the existence of an 8.5 mm/yr sinistral loading rate. If we assume that this rate has been uniform for the past century, the renewal interval would be 125 ± 8 yr. Thus, the 1892 rupture zone at the present time (127 yr after the 1892 earthquake) must be considered sufficiently mature to host an M_w 6.7 earthquake.

Surface slip quantified from InSAR imagery is consistent with variable slip rates along the fault and with postseismic slip associated with nearby $M_w \approx 5$ earthquakes. In 2016, a cluster of these earthquakes occurred near a restraining bend at the southern end of the 1892 rupture (Figs. 1 and 8). Because moderate earthquakes near this segment have not been recorded in the past century, they represent additional concern that a repeat of the 1892 rupture may be approaching.

CONCLUSIONS

Deformed railroads in Balochistan have proven useful in quantifying coseismic slip in earthquakes in 1892 (Griesbach, 1893), 1931 (Szeliga *et al.*, 2009), and 1935 (this article). From surviving historical accounts of the 1892 Chaman earthquake rupture, supplemented by field visits and local enquiries, we deduce that slip and afterslip in 1892 and in the following few years amounted to 1.06 ± 0.07 m. Our estimates are based on a single offset of the fault near the center of its rupture, and hence the deduced value and its uncertainty may not be representative of mean slip in 1892. No detailed mapping of the surface rupture was undertaken at the time of the 1892 earthquake,

Table 1
Inferred Rupture Parameters for the 1892 Chaman Earthquake

Northern End of Rupture		Southern End of Rupture				
Longitude	Latitude	Longitude	Latitude	Slip (m)	Length (km)	M_w
66.58° E	31.03° N	66.38° E	30.60° N	1.06 ± 0.07	51 ± 5	6.7 ± 0.1
Within the defined limits, the fault is formed from several segments with alternating strike.						

and although it may have ruptured from 31.09° N, 66.60° E, north of the Afghan–Pakistan border, to >5 km south of Spin Teza (30.56° N, 66.38° E), a distance of 68 km, a distance that may have been biased in part by the striking morphology of the fault zone rather than by evidence for 1892 offsets, a rupture length closer to 50 km (Table 1) is consistent with observed slip and macroseismic intensity estimates of M_w 6.7. To its south, the rupture terminated within a restraining bend associated with recent seismicity and coincident with a zone of transpressive uplift of the Kwajha Amran mountains.

Recent geodetic datas (GPS and InSAR) suggest that the fault is currently being loaded at approximately 8.5 ± 1 mm/yr (Szeliga *et al.*, 2012), which, if this rate is representative of sinistral slip in the past century, yields a current slip deficit of 1.1 ± 0.1 m, similar to that released in 1892. The recent occurrence (in 2016) of moderate earthquakes near the Kwajha Amran restraining bend additionally signifies that stresses may be approaching levels consistent with imminent future rupture.

DATA AND RESOURCES

Historical data used in this article came from published sources listed in the references. Creep data are archived in UNAVCO. Interseismic Interferometric Synthetic Aperture Radar (InSAR) velocities and fault creep rates shown in Figure 8 are derived from C-band Sentinel-1 Synthetic Aperture Radar (SAR) data collected from October 2014 to March 2019. To ensure high-phase coherence, the geometric and temporal baselines are limited to be less than 150 m and 90 days, respectively. We use the small baseline subset (SBAS) method to solve for the time series and average velocity of line of sight (LoS) displacement at each pixel. We estimate the fault creep rate by differencing the mean LoS velocity of pixels within a 2-km-long and 1-km-wide rectangular box each side of the fault. The differential LoS velocity is then projected to the fault-parallel creep rate assuming no vertical motion across the fault.

ACKNOWLEDGMENTS

The study was initiated during a field study funded by the University of Balochistan, Quetta, in February 2019. The authors thank Nasrullah and Hanifia, residents of Chaman, for their help during the field work. Maps of the Afghan–Pakistan border showing McMahon's mapped fault were researched by Dan Jantzen. W. D. Barnhart was supported by National Aeronautics and Space Administration (NASA) Award NNX16AH53G, and Burgmann and Wang by NASA Award NNX16AL17G.

REFERENCES

Ambraseys, N., and R. Bilham (2003a). Earthquakes in Afghanistan, *Seismol. Res. Lett.* **74,** no. 2, 107–123.

Ambraseys, N., and R. Bilham (2003b). Earthquakes and crustal deformation in northern Baluchistan, *Bull. Seismol. Soc. Am.* **93,** no. 4, 1573–1605.

Ambraseys, N. N., and J. Douglas (2004). Magnitude calibration of north Indian earthquakes, *Geophys. J. Int.* **159,** 165–206.

Anonymous (1893). Effect of an earthquake on a railway, *Railway Rev.* **33,** no. 7, 97.

Anonymous (1909). Letters on the Baluch-Afghan Boundary Commission of 1896, in *The Times of India, Bombay and the Englishman, Calcutta*, A. H. McMahon (Editor), Baptist Mission Press, Kolkata, India.

Baker, T. (1850). *Rudimentary Treatise on Land and Engineering surveying, (The Method of Laying Out Railway Curves on the Ground*, First Ed., John Weale, London, United Kingdom, 136 pp.

Barnhart, W. D. (2017). Fault creep rates of the Chaman fault (Afghanistan and Pakistan) inferred from InSAR, *J. Geophys. Res.* **122,** 372–386, doi: 10.1002/2016JB013656.

Bilham, R., H. Ozener, D. Mencin, A. Dogru, S. Ergintav, Z. Cakir, A. Aytun, B. Aktug, O. Yilmaz, W. Johnson, and G. Mattioli (2016). Surface creep on the North Anatolian Fault at Ismetpasa, Turkey, 1944–2016, *J. Geophys. Res.* **121,** 7409–7431, doi: 10.1002/2016JB013394.

Burrard, S. G. (1915). *Map 34 K/1 Kandahar Province, Chagai District*, scale 1:63,360, Survey of India, Kolkata, India.

Crupa, W. E., S. D. Khan, J. Huang, A. S. Khan, and A. Kasi (2017). Active tectonic deformation of the western Indian plate boundary: A case study from the Chaman Fault System, *J. Asian Earth Sci.* **147,** 452–468, doi: 10.1016/j.jseaes.2017.08.006.

Davison, C. (1893). A note on the Quetta earthquake of 1892, *Geol. Mag.* **10,** no. 3, 356–360.

Egerton, R. W. (1893). Effects of earthquakes in north western railway, India, *Engineering* (19 May 1892) **55,** 698–699.

Fattahi, H., and F. Amelung (2016). InSAR observations of strain accumulation and fault creep along the Chaman Fault system, Pakistan and Afghanistan, *Geophys. Res. Lett.* **43,** 8399–8406, doi: 10.1002/2016GL070121.

Furuya, M., and S. P. Satyabala (2008). Slow earthquake in Afghanistan detected by InSAR, *Geophys. Res. Lett.* **35,** doi: 10.1029/2007GL033049.

Griesbach, C. L. (1893). Notes on the earthquake in Baluchistan on the 20 December 1892, *Rec. Geol. Surv. India*, Part 2, 57–61.

Haq, S., and D. M. Davis (1997). Oblique convergence and the lobate mountain belts of western Pakistan, *Geology* **25,** no. 1, 23–26.

Jackson, W. H. (1895). *Station at Sanzal. Chaman Pakistan, 1895*, Library of Congress photographic collections, Lantern slide 3.25 x 4 in.[LC-W7- 410 [P&P)].

Khan, A. S., S. D. Khan, and D. M. Kakar (2013). Land subsidence and declining water resources in the Quetta Valley, Pakistan, *J. Environ. Earth Sci.* **70,** 2719–2727, doi: 10.1007/s12665-013-2328-9.

Lawrence, R. D., and R. S. Yeats (1979). Geological reconnaissance of the Chaman Fault in Pakistan, in *Geodynamics of Pakistan*, A. Farah and K. A. De Jong (Editors), Geological Survey of Pakistan, Quetta, Pakistan, 351–357.

Lawrence, R. D., S. H. Khan, K. A. De Jong, A. Farah, and R. S. Yeats (1981). Thrust and strike-slip fault interaction along the Chaman transform zone, Pakistan, in *Thrust and Nappe Tectonics*, Spec. Publ. Geol. Soc., London, United Kingdom, 363–370.

Lawrence, R. D., S. H. Khan, and T. Tanaka (1992). Chaman fault, Pakistan–Afghanistan, in *Major Active Faults of the World, Results of IGCP Project 206*, R. Buckham and P. Hancock (Editors), Annales Tect. 6 (Suppl.), Universitá di Firenze, Dipartimento di scienze della terra, Firenze, Italy, 196–223

Lienkaemper, J. L., and F. S. McFarland (2017). Long-term afterslip of the 2004 M 6.0 Parkfield, California, earthquake—Implications for forecasting amount and duration of afterslip on other major creeping faults, *Bull. Seismol. Soc. Am.* **107,** no. 3, 1082–1093, doi: 10.1785/0120160321.

McMahon, A. H. (1897). The southern borderlands of Afghanistan, *Geograph. J.* **9,** no. 4, 392–416.

Skrine, C. P. (1936). The Quetta earthquake, *Geogr. J.* **88,** 414–428.

Szeliga, W., R. Bilham, D. M. Kakar, and S. H. Lodi (2012). Interseismic strain accumulation along the western boundary of the Indian

subcontinent, *J. Geophys. Res.* **117,** no. B08404, doi: 10.1029/2011JB008822.
Szeliga, W., R. Bilham, D. Schelling, D. M. Kakar, and S. Lodi (2009). Fold and thrust partitioning in a contracting fold belt: Evidence from the 1931 Mach Earthquake in Baluchistan, *Tectonics* **28,** doi: 10.1029/2008TC002265.
Thingbaijam, K. K. S., P. M. Mai, and K. Goda (2017). New empirical earthquake source-scaling laws, *Bull. Seismol. Soc. Am.* **107,** no. 5, 2225–2246, doi: 10.1785/0120170017.
Ul-Hadi, S., S. D. Khan, L. Owen, and A. S. Khan (2013). Geomorphic response to an active transpressive regime: A case study along the Chaman strike-slip fault, western Pakistan, *Earth Surf. Process. Landf.* **38,** 250–264, doi: 10.1002/esp.3272.
Ul-Hadi, S., S. D. Khan, L. A. Owen, A. S. Khan, K. A. Hedrick, and M. W. Caffee (2013). Slip-rates along the Chaman fault: Implication for transient strain accumulation and strain partitioning along the western Indian plate margin, *Tectonophysics* **608,** 389–400.
West, W. D. (1935). Preliminary geological report on the Baluchistan (Quetta) earthquake of May 31st 1935, *Rec. Geol. Surv. India, 69*, 203–240.
Wheeler, E. O. (1941). *Map 34 K, Kandahar Province, Chagai and Quetta Pishin Districts and Kalat state*, Survey of India, Kolkata, India, scale 1:253,400.
Yeats, R. S., R. D. Lawrence, S. Jamil-ud-Din, and S. H. Khan (1979). Surface effects of the 16 March 1978 earthquake, Pakistan–Afghanistan border, in *Geodynamics of Pakistan*, A. Farah and K. A. De Jong (Editors), Geologic Survey of Pakistan, Quetta, Pakistan.

Roger Bilham
CIRES and Department of Geological Sciences
University of Colorado
Boulder, Colorado 80302 U.S.A.
bilham@colorado.edu

Najeeb Ullah Kakar
Din Mohammad Kakar
Faculty of Earth and Environmental Sciences
Department of Geology
University of Balochistan
Quetta 87550, Pakistan

Kang Wang
Roland Bürgmann
Department of Earth and Planetary Science
University of California
Berkeley, California 94720 U.S.A.

William D. Barnhart
Department of Earth and Environmental Sciences
University of Iowa
Iowa City, Iowa 52240-9071 U.S.A.

Published Online 25 September 2019